Heat and Technology
Vol. 32, n. 1-2, 2014

HYBRID ANALYTICAL TECHNIQUE THERMAL MODELING OF GAS INSULATED TRANSMISSION LINE

Jehan H. Shazly, Magdy B. Eteiba, and Yasser M. El-Sayed

Department of Electrical Engineering, Fayoum University, Egypt

ABSTRACT

The gas-insulated transmission line (GIL), which is a replacement of an overhead line in some special environments has been used because of its high capacity, low losses and no electromagnetic interference. A mathematical thermal model for predicting the steady state temperature distribution inside and outside GIL is investigated by merging two techniques to get rid of using sensors inside the GIL cable. The finite element analysis involving formulation and solution of the heat conduction equations has been done. During the solution of the heat conduction equations of the proposed model, a numerical study based on energy conservation equation using MATLAB programming is performed to determine the bulk temperatures of SF_6 gas inside the cable. The calculated values are verified with experimentally measured values under the same conditions and both show close agreement with each other.

1. INTRODUCTION

One of the fundamental considerations, which limit the cable load ability and usable life, is determined by its ability to dissipate the internally generated heat to its surroundings. It is therefore essential to predict thermal behaviors of a cable during normal operating conditions and particularly in the presence of overload conditions. Furthermore, the improved knowledge of cable thermal characteristics can allow engineers to achieve enhanced designs and manufacturers are particularly interested in its accurate prediction.

The GIL offers an opportunity to transmit large amounts of electrical energy over long distances. Moreover, they do not require supplementary cooling and can be run over distances more than 30 km without additional power factor correction [1]. They also have low transmission losses, low capacitive load, no electric ageing, no thermal ageing and power rating like an overhead line [2]. In addition, because of using compressed SF_6 gas and metal enclosure, the effect of electromagnetic interference of GIL is none.

This paper proposes hybrid numerical techniques for GIL power cable thermal modeling, combining the benefits of the heat conduction equation using finite element analysis and the energy balance equations using differential equations to determine the bulk temperature of fluid inside the cable without needing to measuring tools of temperatures.

The steady-state thermal performance of GIL cable due to conditions imposed on its boundaries is considered [3]. The convective and radiative heat transfers boundary conditions are completely dominant in the present study. Different loading, ambient temperature, and cooling conditions have also been considered. The numerical simulation of the heat transfer by conduction equation was carried out with ANSYS 13, which is a general-purpose finite-element method based software package for heat transfer problems, and MATLAB programming in order to solve ordinary, first-order, nonlinear, and non-homogenous differential equations of energy balance equations.

The GIL system will be 3-phase power line geometric flat formation insulated with pure SF_6 gas, located in free air. A full description of the thermal model is presented. The factors effect on the model such as changes of load, gas pressure, ambient temperature, wind velocity, and radiation effects are studied. The predicted temperatures are compared with experimentally measured values under the same conditions.

2. METHODOLOGY

In the case of GIL cables, an important issue is the operating temperature and indeed the thermal history of the cable. Numerical steady-state thermal analysis of an electrical power cable system placed in free air is presented in this work. The thermal system is divided into two parts; the GIL cable and the surrounding air, looking physics phenomena occurring in each one.

GIL cable in our study consists of two concentric aluminum tubes the inner conductor and the outer enclosure. This enclosure is formed by a sturdy aluminum tube, which provides a solid mechanical and electro-technical containment for the system. GIL is filled with an insulating SF_6 gas. It has been assumed that the GIL is too long. Therefore, with a reasonable acceptable accuracy, the three-dimensional (3-D) problem is reduced to a two-dimensional (2-D) one with X and Y as space variables as shown in Figure 1. Inside the cable, the finite-element method divides the solution domain into simply shaped regions, or elements, as demonstrated in Figure 1. The material properties and the governing relationships are considered over these elements.

The heat differential equation is performed on each element of the GIL. By gathering, the individual solutions to ensure continuity at the inter-element boundaries, the total solution is then calculated. The analysis of heat conduction

problem needs a suitable boundary. The boundary conditions are the set of conditions specified for behavior of the solution to a set of differential equations at the boundary of its domain.

The theoretical thermal model for the type of the GIL developed here is limited by the following basic assumptions: 3-phase power line geometric flat formation is assumed moreover, one phase will be analyzed for the simplicity, neglecting the mutual effect. The heat generated per unit volume of the conductor aluminum tubes is uniformly distributed in it. The dielectric losses caused by the voltage across the insulation are neglected due to the small capacitance of SF_6 gas. The enclosure losses are assumed to be small compared to conductor losses, so it is not taken into account. The convection and radiation of SF_6 gas inside the conductor is neglected. Only measured values of ambient temperature are always considered. The physical properties of all materials in the cable system are temperature dependent, and can be found in [4,5].

In this paper, we present a finite element thermal analysis study of heat transfer (using ANSYS 13) inside and outside the GIL to obtain steady state temperature distribution of this kind of GIL system at any specified location.

The heat conduction for steady state heat transfer of 2-D model is governed by Eq.(1) [6,7,11]. This loading condition is a situation where heat storage effects varying over a period of time can be ignored.

$$\frac{d}{dx}\left(K\frac{dT}{dx}\right)+\frac{d}{dy}\left(K\frac{dT}{dy}\right)+W=0 \quad (1)$$

Where T is temperature in (K), x and y are spatial variables in (m), K is the thermal conductivity in (W/m K), W is the heat transfer rate in (W/m^3).

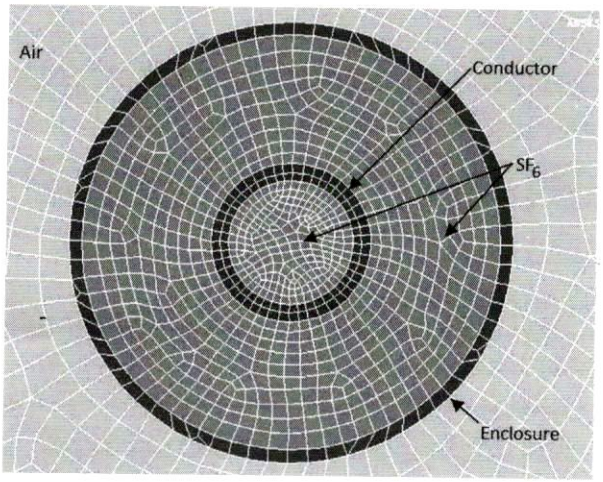

Figure 1 Schematic of GIL cable with elements layout for finite element formulation.

All the losses occurring in the conductor are converted into heat. This heat is transferred to the air surrounding the GIL due to a temperature difference at the boundaries. First, the transfer of heat starts from the inside of the conductor and expands to its external surface which is submerged in the SF_6 gas, by heat conduction. Then, the heat is transferred from the conductor outside surface to the gas by convection. In addition, there is a thermal radiation between the conductor outside surface and the inner surface of the enclosure. Next, the heat is transferred by convection from the gas to the inner surface of the enclosure. Then, the heat energy is transmitted through the thickness of the enclosure by conduction. The last stage is the heat dissipation by convection and radiation from the external surface of the enclosure to the surrounding air.

2.1 Power Loss in the Cable

The heat generated per unit volume of the aluminum conductor is caused by the conductor current passing through the resistance of it [9]. The power loss in the cable is calculated according to equations from Eq.(2) to Eq.(5).

$$W = W_c \text{ (W/m)/ area of the conductor } (m^2) \quad (2)$$

$$W_c = I^2 R \quad (3)$$

$$R = R'(1+y_s+y_p) \quad (4)$$

$$R' = \frac{1.02\times10^6\rho_{20}}{S}[1+\alpha_{20}(T-20)] \quad (5)$$

Where, I is the cable current. W_c (W/m), R (Ω/m) and R' (Ω/m) are the conductor's losses, ac resistance and dc resistance, respectively. ys and yp are skin effect and proximity effect, respectively. S (mm^2) is the cross-sectional area of conductor. T (°C) is the conductor temperature. ρ_{20} is the resistivity for aluminum at 20 °C, and α_{20} is the temperature coefficient for aluminum at 20 °C.

Several convective and radiative heat transfer coefficients must be evaluated in order to determine the temperatures of the cable components.

2.2 Convection Boundary Conditions

The convection means that the heat transfer will occur between a surface and a moving fluid when they are at different temperatures. Here in our GIL model, the heat is transferred by convection between the conductor outer surface and the SF_6 gas flowing over it, from the SF_6 gas to the inner surface of the enclosure, and finally from the external surface of the enclosure to the surrounding air.

By considering an energy balance at the surface, the mathematical formulation of this convection boundary condition is as Eq.(6) [8].

$$-\left(K\frac{dT}{dx}\right)-\left(K\frac{dT}{dy}\right)=h(T-T_B) \quad (6)$$

Where h is the convective heat transfer coefficient in (W/K m^2) and it can be determined by classical Nusselt number (N_u) correlation's as Eq.(7) [7]. T_B is the bulk temperature that is determined based on energy balance equation using MATLAB programming and will be clarified later.

$$h=\frac{K}{D}N_u \quad (7)$$

Where, D (m) is the diameter of the tube. The characteristic dimension D depends on the calculation place (outer diameter of conductor, inner diameter of enclosure, and outer diameter of enclosure). It should be noted that the convective heat transfer coefficients are based on the assumption that only natural convection is present inside the power cable. Natural or forced convection occurs as a result of air circulation outside the GIL with wind.

The average Nusselt number for Free convection between the outer surface of the conductor and the surrounding SF_6 gas, given by equations Eq.(8) and Eq.(9) [10]:

$$N_u = \frac{2}{ln\left[1+\frac{2}{N_{ui}}\right]} \tag{8}$$

$$N_{ui} = \left[\left(0.649{R_a}^{1/4}\left[1+\left(\frac{0.559}{P_r}\right)^{3/5}\right]^{-5/12}\right)^{15} + \left(0.12{R_a}^{1/3}\right)^{15}\right]^{1/15} \tag{9}$$

The dimensionless parameters of free convection such as Rayleigh number (R_a), Prandtl number (P_r), as well as coefficient of thermal expansion, are demonstrated in [10].

The average Nusselt number for Free convection between the SF_6 gas and the inner surface of the enclosure, given by the equations Eq.(10), Eq.(11) and Eq.(12) [10]:

$$N_u = \frac{-2}{ln\left[1-\frac{2}{N_{ui}}\right]} \tag{10}$$

$$N_{ui} = \left[\left(0.587G{R_a}^{1/4}\right)^{15} + \left(0.12{R_a}^{1/4}\right)^{15}\right]^{1/15} \tag{11}$$

$$G = \left[\left(1+\frac{0.6}{{P_r}^{0.7}}\right)^{-5} + \left(0.4+2.6{P_r}^{0.7}\right)^{-5}\right]^{-1/5} \tag{12}$$

The convective heat transfer coefficient between the outer surface of the enclosure of the cable and the air is based on the assumption that only forced convection due to air circulation outside the cable by wind effect is considered. Otherwise it is considered as free convection.

The average Nusselt number by free convection given by Eq.(13) [10]:

$$N_u = \left[0.6+\frac{0.387{R_a}^{1/6}}{\left[1+\left(\frac{0.559}{P_r}\right)^{9/16}\right]^{8/27}}\right]^2 \tag{13}$$

The average Nusselt number by forced convection given by Eq.(14) [9]:

$$N_u = C_1 {R_e}^m \tag{14}$$

The dimensionless parameter of forced convection as Reynolds number (R_e) is presented in [9], where the values of C_1 and m shown in [11] based on the flow pattern of (R_e).

2.3 Radiation Boundary Condition

Transmission of the energy by the electromagnetic wave called radiation. Radiation analyses are highly nonlinear because the heat flow that causes radiation varies with the fourth power of the absolute temperature, [4,10].

The radiation effects appear in the heat transfer analysis only through the boundary conditions. In this model, two types of enclosure surfaces participated in the radiation process are considered in our model. The closed type enclosure radiates heat between the outside surfaces of the conductor and the inner surface of the enclosure. The open type enclosure surface was assumed between the external surface of the enclosure and the surrounding air with known ambient temperature. The characteristics of each radiating surface of an emissivity value and a direction of radiation assigned to it.

The differential equation governing the radiation energy is obtained by considering an energy balance at the surface stated as Eq.(15) [4,8,10].

$$-\left(K\frac{dT}{dx}\right)-\left(K\frac{dT}{dy}\right) = \sigma\varepsilon F_{ij}\left(T^4-{T_B}^4\right) \tag{15}$$

Where σ is Stefan-Boltzman constant. ε is the infrared emissivity, T_B is the bulk temperature which is determined based on energy balance equation using MATLAB programming and the F_{ij} view factor . It is defined as the fraction of the radiation that leaves the surface A_i and is intercepted by the surface A_j. The view factor can be obtained from Eq.(16) [10].

$$F_{ij} = \frac{1}{A_i}\int_{A_i}\int_{A_j}\frac{cos\theta_i cos\theta_j}{\pi R^2}\,dA_i dA_j \tag{16}$$

Elemental areas on each surface, dA_i and dA_j, are connected by a line of length R, which forms the polar angles θ_i and θ_j, respectively. The values R, θ_i and θ_j vary with the position of the elemental areas (m^2) on A_i and A_j.

2.4 Bulk Temperature

The bulk temperatures which are needed to calculate the convective and radiative heat transfer coefficients in the finite element analysis involving formulation and solution of the heat conduction equations for the outside surface of the conductor and the inner surface of the enclosure must be known. In this model, only measured ambient temperature is always considered, no other sensors are used to know the bulk temperature of the insulating SF_6 gas.

As a result of subdividing the cable into the three major components: the conductor; SF_6 gas; the enclosure. The basic energy conservation equations under steady state conditions for the cable system using MATLAB programming are applied for each cable's component. The model is capable of determining only the average temperature of each component, which is used to obtain the bulk temperatures for outside surface of the conductor and inside surface of the enclosure in order to use these bulk temperatures to calculate the different convective and radiative heat transfer coefficient in finite element analysis.

There are three unknown temperatures, the conductor temperature (T_c), the SF_6 gas temperature (T_g), and the enclosure temperature (T_s). These temperatures are thus computed from the following three equations Eq.(17), Eq.(18), and Eq.(19).

Steady state energy balance on the conductor could be written as:

$$W_c = h_c A_c\left(T_c-T_g\right)+\sigma A_c F_{cs}\left({T_c}^4-{T_s}^4\right) \tag{17}$$

Steady state energy balance on the insulating gas yields:

$$h_c A_c\left(T_c-T_g\right) = h_{si} A_{si}\left(T_g-T_s\right) \tag{18}$$

Steady state energy balance on the outer sheath or enclosure may be expressed as:

$$\sigma A_c F_{cs}\left({T_c}^4-{T_s}^4\right)+h_{si}A_{si}\left(T_g-T_s\right) = \sigma A_{so}\varepsilon_a\left({T_s}^4-{T_a}^4\right)+h_{so}A_{so}\left(T_s-T_a\right) \tag{19}$$

Where the subscript "c" refers to a property of the conductor, "g" refers to a gas property, "s" refers to a property of the enclosure, and the subscript "a" indicates a property of the

ambient air. Where "*i*" and "*o*" indicates to inside and outside respectively.

The gas bulk temperature at the outside surface of the conductor is the average of T_c and T_g that calculated in MATLAB. The gas bulk temperature for the inner surface of the enclosure is the average temperature of T_c and T_s which estimated in MATLAB.

3. RESULTS AND DISSCUSION

A steady-state analysis has been applied for the prediction of the thermal performance of GIL cable at various ratings, operating under different loading conditions and its results were validated by comparing the computed temperatures with the measured results reported in [11].

The selected system consists of a flat horizontal coaxial configuration 3-phase, 500 kV and 7000 A at full load, with the conductor's inner diameter of 0.14 m and outer diameter of 0.18 m, The enclosure's inner diameter of 0.470 m and the outer diameter of 0.5 m. Both the conductor and the enclosure are made of aluminum alloy (A6063-T5). The conductor's outer surface and the inner surface of the enclosure are treated with black Almite with an infrared emissivity coefficient of 0.9. The enclosure outer surface was painted with (Munsell N7) with infrared emissivity coefficient of 0.8 [11].

3.1 Full Load

The Thermal model was verified using ANSYS 13 finite-element analysis program and MATLAB programming. The accuracy of the numerical results, which are obtained from the thermal analysis, was verified by comparing the computed results with the measured values reported in [11].

The recorded outside top of conductor temperature was 49 °C, the measured gas temperature was 35 °C and the recorded outside top of enclosure temperature was 24.5 °C at an ambient temperature of 23 °C, and with gas pressure (3.5 kg/cm^2 at 20 °C) during full load (7000 A), which was reported in [11]. The present model has been examined at these conditions. The predicted contour plot for a nodal temperature distribution of the GIL power cable at full load (7000 A) is shown in Figure 2.

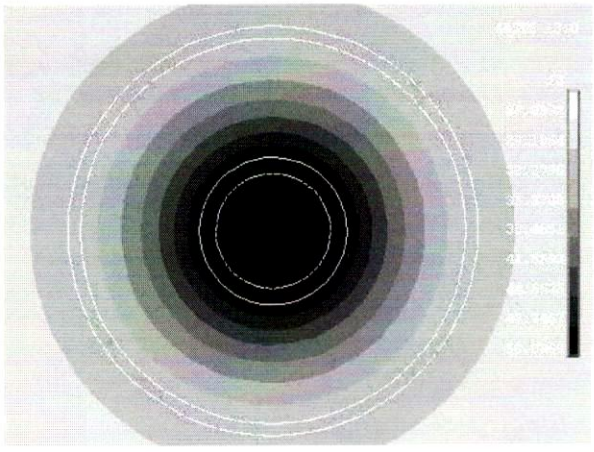

Figure 2 Calculated temperature distribution at full load.

The calculated results of the GIL cable component temperatures versus the radius of the cable are illustrated in Figure 3. It can be observed that the conductor temperature varies between 50.839 °C and 50.814 °C. The gas temperatures measurements were recorded in the region between the conductor and the enclosure. The gas temperature varies between 47.745 °C and 31.63 °C. Thus, the top gas temperature was assumed at the layer near the outer conductor surface and far about 2 cm from the surface of the conductor and it can be considered as 45.92 °C. The enclosure temperature varies between 30.025 °C and 30.016 °C. Therefore, it can be noticed that there is a good agreement between the calculated temperatures and the measured temperature values reported by [11].

In the following sections, different evaluations are carried out assuming different characteristics for the GIL cable design parameters and the climatic conditions, and comparing results against those of a base case, illustrated in Figure 2, and Figure 3.

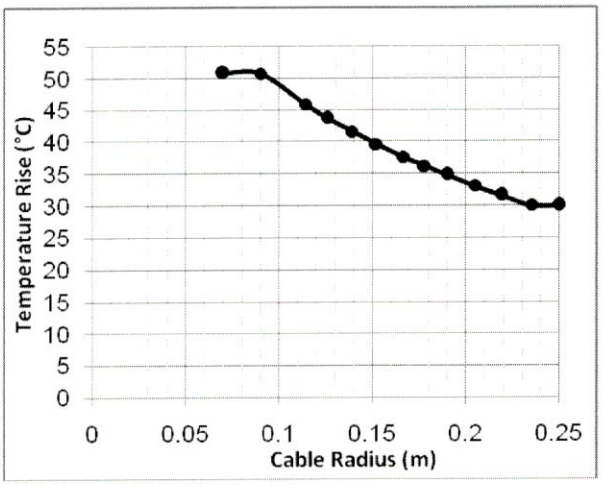

Figure 3 Variation of calculated temperature of the cable at full load versus the radius of the cable.

3.2 Over Load

The cable temperatures during over load are one of the most important aspects that determine the aging rate of the insulation. For GIL over loading at (8000 A), the recorded outside top of conductor temperature was 60.5 °C, the recorded gas temperature was 42.5 °C, and the recorded outside top of enclosure temperature was 30 °C at an ambient temperature of 25 °C, and with gas pressure (3.5 kg/cm^2 at 20 °C), which was also reported in [11].

A typical contour plot for a nodal temperature distribution in the GIL cable at over load (8000 A) is shown in Figure 4. The results of the predicted GIL cable component temperatures versus the radius of the cable compared to the reference case are displayed in Figure 5. Compared with the reference case, it can be noticed at over load (8000A) that, the conductor temperature varies between 61.193 °C and 61.16 °C. The gas temperatures measurements were recorded in the region between the conductor and the enclosure. The gas temperature varies between 57.17 °C and 36.578 °C thus; the top gas temperature is 54.922 °C. The enclosure temperature varies between 34.509 °C and 34.496 °C. It can be seen that

the recorded measured temperatures [11] agree with the calculated results. It can also be recognized that, when the load power increased, the temperatures of the cable components are also increased.

Compared with the reference case at full load (7000 A), the influence of increasing the load is greatest on the conductor temperatures with a typical value of about 10.354 °C. The top gas temperatures were affected to lesser degree with an increase of 9 °C recorded. The least effect was observed in the enclosure temperatures with a typical increase of 4.484 °C. This may be due to the fact that the heat generated per unit volume per unit time of the conductor increase with the increase of load so the most heated part is concentrated in the conductor.

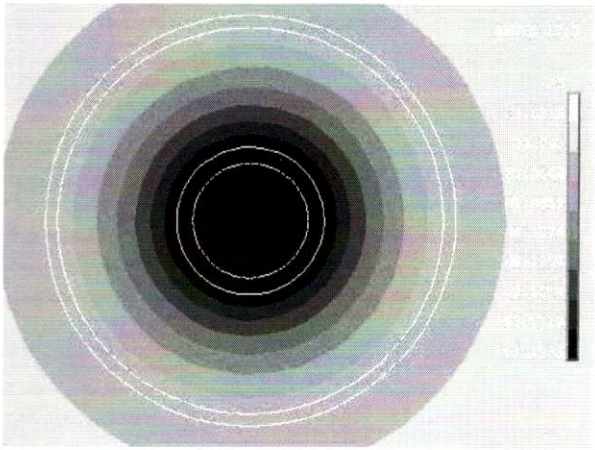

Figure 4 Calculated temperature distribution at overload of (8000 A).

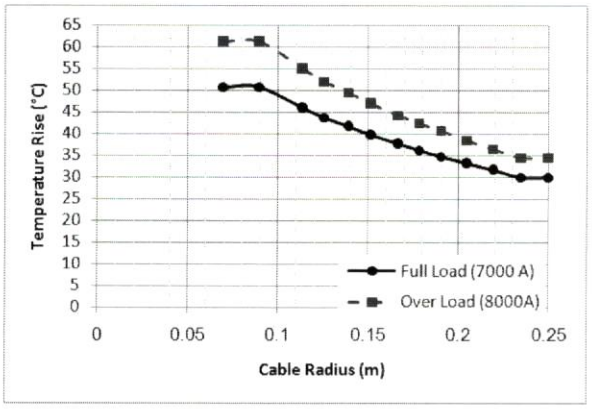

Figure 5 Effect of over load (8000A) on cable temperatures Compared with the reference case (7000A).

3.3 Increasing SF_6 Gas Pressure at Full Load

To determine the effect of increasing the pressure of SF_6 gas on the GIL cable component temperatures, the reference case was re-evaluated for (4.5 kg/cm^2 at 20 °C) SF_6 gas pressure at full load (7000 A) and at ambient temperature of 23 °C.

The predicted contour plot for a nodal temperature distribution for the GIL cable at full load (7000 A) and 4.5 kg/cm^2 is illustrated in Figure 6. It can be seen that the conductor temperature varies between 49.065 °C and 49.041 °C. The gas temperatures measurements were recorded in the region between the conductor and the enclosure. The gas temperature varies between 46.16 °C and 31.704 °C. Thus, the top gas temperature was assumed at the layer near the outer conductor surface and far about 2 cm from the surface of the conductor and it can be considered as 44.609 °C. The enclosure temperature varies between 30.261 °C and 30.252 °C.

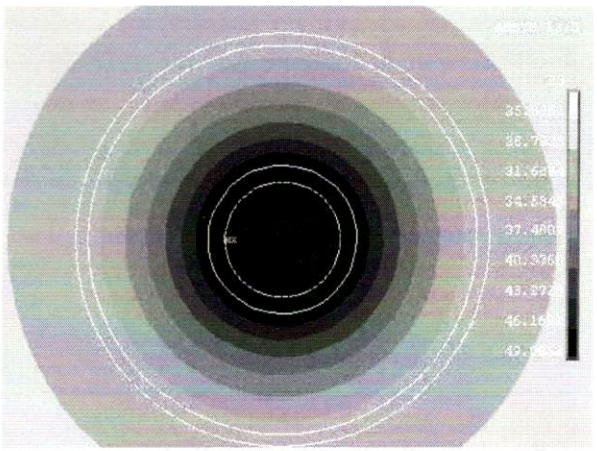

Figure 6 Calculated temperature distribution at full load with SF_6 gas pressure of 4.5 kg/cm^2.

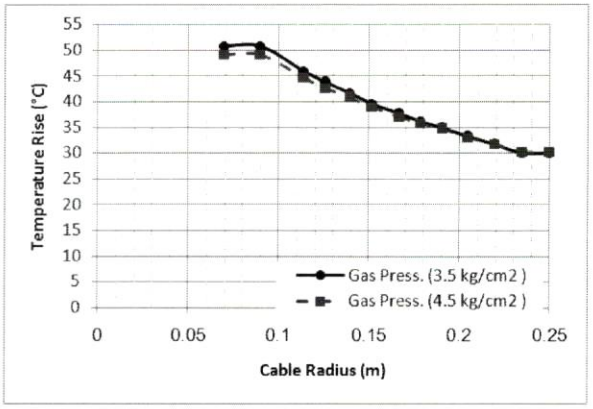

Figure 7 Effect of increasing SF_6 gas pressure on cable temperatures compared with the reference case (7000 A).

Details of comparison made between the predicted cable temperatures of the reference case and the case of increasing the gas pressure to (4.5 kg/cm^2 at 20 °C) versus the radius of the cable is represented in Figure 7. It can be noticed that, the GIL cable component temperatures decrease with an increase

in SF_6 gas pressure because the increase in gas pressure causes an improvement in thermal capacity because the increase in gas pressure causes an increase in SF_6 gas density, and a decrease in the kinematic viscosity of the gas.

The Nusselt number of SF_6 gas is influenced by the change of kinematic viscosity which is dependent on the gas pressure. Therefore, the temperatures of the cable under high gas pressure are lower than those under low filled gas pressure.

3.4 For Ambient Temperature Changes

To investigate the profile of the cable component temperatures at different ambient temperatures, the system was examined at two other conditions of ambient temperatures: 45 °C, and zero °C at full load (7000 A) and SF_6 gas pressure of (3.5 kg/cm^2 at 20 °C).

The temperature distribution of the GIL cable system, of the basic case at ambient temperature of 23 °C, is plotted in Figure 2.

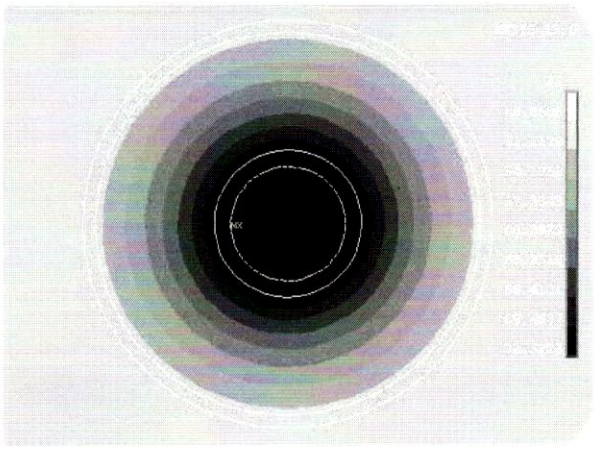

Figure 8 Calculated temperature distribution at full load at ambient temperature of 45 °C

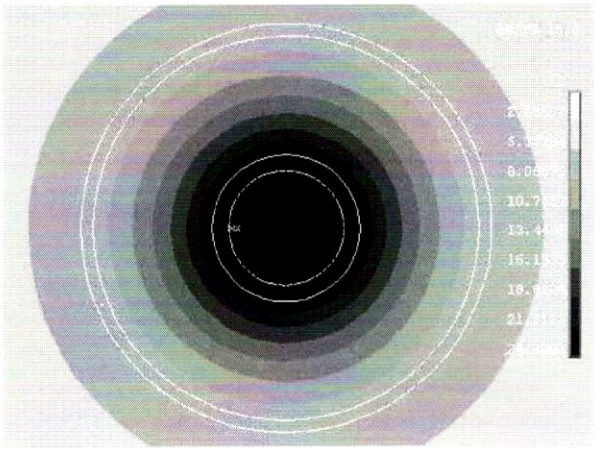

Figure 9 Calculated temperature distribution at full load at ambient temperature of 0 °C.

The results at ambient temperatures of 45 °C and zero °C are illustrated in Figure 8, and Figure 9, respectively. It can be noticed that, the cable temperatures increase as the ambient temperature increases and vice versa.

The calculated GIL cable component temperatures versus the radius of the cable at full load for the three different ambient temperatures of the conductor, the SF_6 gas, and the enclosure are shown in Figure 10. The estimated results confirm the significant influence of the ambient temperature on the GIL cable component temperatures. The thermal properties of the power cable are affected as expected by the environmental conditions.

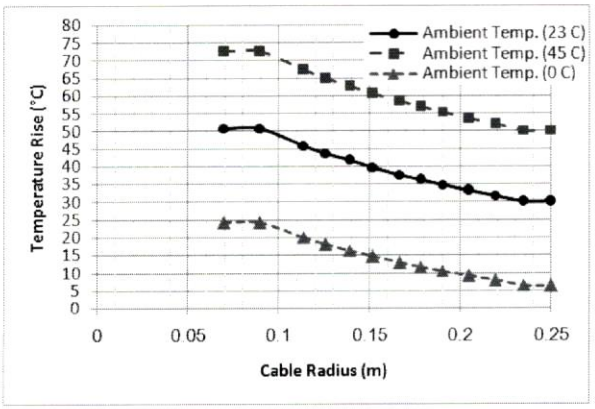

Figure 10 The cable temperatures against the changes of the ambient temperatures.

3.5 For Wind Velocity Changes

The effect of varying wind velocity on the cable component temperatures was investigated. The response of the GIL system of the basic case at no wind effect is as shown in Figure 2. The simulation was carried out at 5 m/s air velocity during full load (7000A), at an ambient temperature of 23 °C, and with gas pressure (3.5 kg/cm^2 at 20 °C). The wind speed represents the forced convection in our model.

Figure 11 displays the temperature distributions of the GIL cable with the effect of wind velocity at 5 m/s. the conductor temperature varies between 44.059 °C and 44.034 °C. The gas temperatures measurements were recorded in the region between the conductor and the enclosure. The gas temperature varies between 41.718 °C and 25.663 °C. Thus, the top gas temperature was assumed at the layer near the outer conductor surface and far about 2 cm from the surface of the conductor and it can be considered as 39.345 °C. The enclosure temperature varies between 24.129 °C and 24.121 °C.

The estimated results of the GIL cable component versus the radius of the cable at full load for wind velocity of 5 m/s compared to the reference case of no wind effect is shown in Figure 12. It can be observed that the wind velocity during the forced convection process affects the cable component temperatures. The GIL cable temperatures decrease with an increase in air velocity. The increase in air velocity causes an increase in the Reynolds number, and Nusselt number with a consequent increase in heat transfer coefficient during the forced convection process. The pronounced decrease in the cable component temperatures takes place in the enclosure because it is closely linked to the wind velocity.

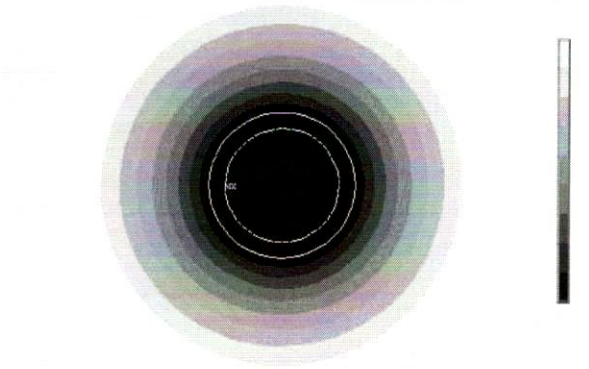

Figure 11 Calculated temperature distribution at full load with wind velocity of 5 m/s.

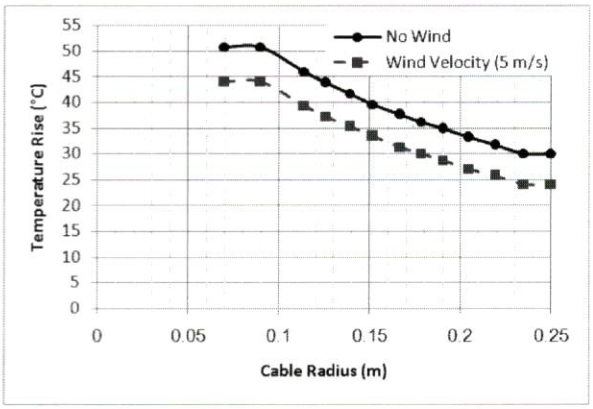

Figure 12 Effect of wind velocity on cable temperatures compared with the reference case (7000 A).

3.6 The Effect of the Infrared Emissivity

The components temperature of the cable can be controlled to a certain extent by changing the type of paint used on the outside surface of the conductor and the inner surface of the enclosure. This will in turn change the value of the infrared emissivity of the type of paint used.

To determine the effect of the infrared emissivity on the GIL cable component temperatures, the reference case which was displayed in Figure 2, was re-evaluated with the value of the infrared emissivity decreased from 0.9 to 0.1 (left unpainted) at full load (7000 A) and SF_6 gas pressure of (3.5 kg/cm^2 at 20 °C) at ambient temperature of 23 °C.

Figure 13 represents the numerical solution of temperature distributions of the cable at low value of infrared emissivity at 0.1. The conductor temperature varies between 56.653 °C and 56.629 °C. The gas temperatures measurements were estimated in the region between the conductor and the enclosure. The gas temperature varies between 52.91 °C and 34.1 °C. Thus, the top gas temperature was considered as 50.901 °C. The enclosure temperature varies between 32.209 °C and 32.197 °C.

The results of the comparison between evaluated GIL cable temperatures of the reference case and the case of infrared emissivity of 0.1 are illustrated in Figure 14. It can be seen that, this increase in the cable component temperatures is due to decreasing the infrared emissivity occurs as a result of reduction in heat transferred to the surrounding.

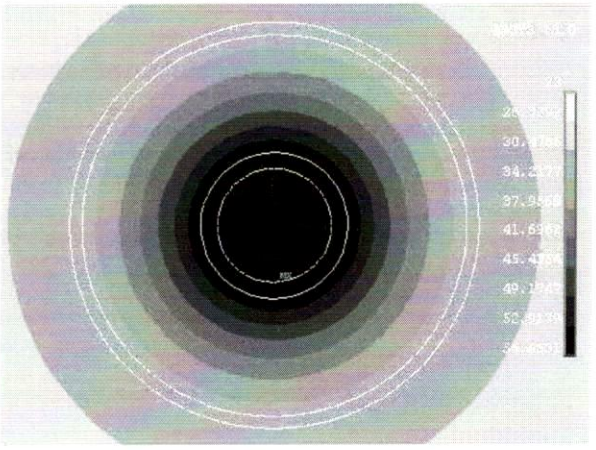

Figure 13 Calculated temperature distribution at full load at infrared emissivity of 0.1.

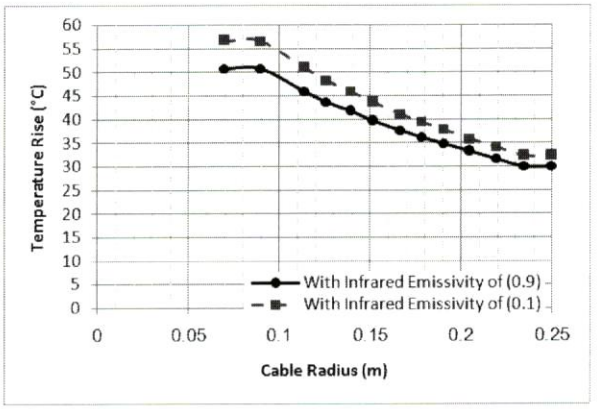

Figure 14 Effect of the different values of infrared emissivity on cable components temperatures.

4. CONCLUSION

The developed thermal model presented in this paper merges between the two basic concepts of heat transfer of heat conduction equation and energy conservation equation in order to get rid of using sensors inside the GIL cable. This theoretical model permits the calculation of the temperatures at any specified location inside and outside the GIL considering the variations in boundary conditions, and the contributions of the convective and radiative heat transfer. The analytical approach for evaluating temperature distribution followed in the present investigation seems to correspond adequately well with results of actual measurements.

Different computations with variation in design and / or environmental parameters provide useful information which can be accessed and manipulated by the GIL cable designer or

operator to simulate, in a simple and efficient manner, various ambient, loading, and boundary variations.

5. REFERENCES

1. O. Volcker, H. Koch, Insulation Coordination for Gas Insulated Transmission Lines (GIL), *IEEE Trans. on Power Delivery,* vol. 16, pp. 122-130, 2001.
2. H. Koch, *Gas-Insulated Transmission Lines (GIL)*, John Wiley & Sons, United Kingdom, 2012.
3. Raoudha Chaabane, Faouzi Askeri, Sassi Ben Nasrallah, Numerical Modelling of Boundary condition for Two Dimentional conduction Heat Transfer Equation Using LATTICA BOLTEZMANN Method, *International Journal of Heat and Technology*, Vol. 28 No. 2, PP. 51-57, 2010.
4. G. D. Raithby, K. G. T. Hollands, *Handbook of Heat Transfer*, third ed., McGraw-Hill, New York, 1998.
5. Ines Boulaoued, Faycel Khemili, Abdallah Mhimid, Therml Characterization of Insulating Materials, *International Journal of Heat and Technology*, Vol. 30 No. 2, PP. 63-68, 2012.
6. J. N. Reddy, D. K. Gartling, *Finite Element Method in Heat Transfer and Fluid Dynamic*, second ed., CRC Press, FL, 2000.
7. M. N. Ozisik, *Heat Transfer a Basic Approach*, McGraw- Hill, New York, 1985.
8. M. B. Eteiba, M. M. Abdel Aziz, J. H. Shazly, Heat Conduction Problems in SF_6 Gas Cooled-Insulated Power Transformers solved by the Finite-Element Method, *IEEE Trans. on Power Delivery,* vol. 23, pp. 1457-1463, 2008.
9. G. J. Anders, *Rating of Electric Power Cables in unfavorable Thermal Environment*, John Wiley & Sons, United Kingdom, 2005.
10. M. B. Eteiba, Steady State and Transient Ampacities of Gas-Insulated Transmission Lines, *IEEE MELECON*, pp. 424-428, 2002.
11. D. Minagushi, M. Ginno, K. Itaka, H. Furukawa, K. Ninomiya, T. Hayashi, Heat Transfer Characteristics of Gas Insulated Transmission Lines, *IEEE Trans. on Power Delivery,* vol. 1, pp. 2-9, 1986.

NOMENCLATURE

C	Specific heat, (J/kg K)
D	Length, (m)
Gr	Grashof number, dimensionless.
h	Convective heat transfer coefficient,(W/m^2 °C)
I	Cable current (A)
K	Thermal conductivity, (W/m K)
N_u	Nusselt number, dimensionless
P_r	Prandtl number, dimensionless
q	Generated heat, (Watt)
R_a	Rayleigh number, dimensionless
R_e	Reynolds number, dimensionless
R	AC value of conductor resistance (ohm/m)
R'	DC value of conductor resistance (ohm/m)
T	Temperature, (°C)
T_B	Bulk temperature of the adjacent fluid, (°C)
W_c	The conductor losses (W).
y_s	Skin factor
y_p	Proximity factor

Greek Symbols

ε	Infrared emissivity, dimensionless.
σ	Stephen–Boltzman constant,$5.67\ 10^{-8}$,($W/m^2\ °K^4$)
ρ	Density, (kg/m^3).